NUMERICAL STUDY OF SATURATION STEAM/WATER MIXTURE FLOW AND FLASHING INITIAL SUB-COOLED WATER FLOW INSIDE THROTTLING DEVICES

Quang Dang Le, Riccardo Mereu, Giorgio Besagni, Vincenzo Dossena, Fabio Inzoli

Politecnico di Milano, Department of Energy

email: lequang.dang@polimi.it

CERN – Geneva, September 21-23 2016

OUTLINE

- Introduction
- State-of-the-art
- Experimental benchmark
- Numerical modeling
- Results
- Final remarks

INTRODUCTION

MOTIVATION

➢ Phase change driven by pressure has a wide application in industrial application (control valve, safety valve and ejector, etc)

➢ Phenomenon inside throttling devices is very complicated due to Thermal (boiling delay) and mechanical (slip between two phases) non-equilibrium effects

OBJECTIVE

➢ Comprehensive understand about **thermal non-equilibrium** effect and **mechanical non-equilibrium** effect inside nozzle.

➢ **Generate reliable data** to validate and develop exisiting sizing formulas

- Omega method – J. C. Leung (Equilibrium flow)
- HNE-DS – Prof. Jurgen Schmidt (Non-equilibrium flow)
- …

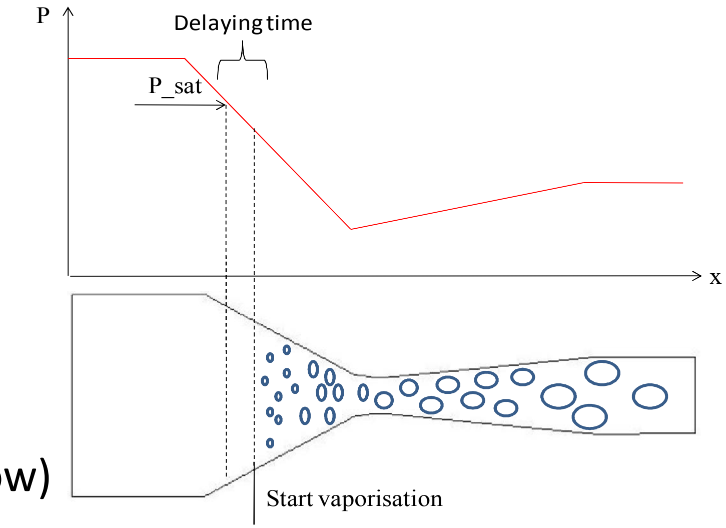

INTRODUCTION

Main **goals** of the COMPUTATIONAL FLUID DYNAMICS (CFD) analysis

- validate the CFD model, providing guidelines on CFD simulations
- Understand physical behaviors of phase change driven by pressure with non-equilibrium effects inside throttling devices
- Compare with other CFD model for modeling flash boiling flow with non-equilibrium effects

STATE-OF-THE-ART

- **Experimental studies**

  - Mass flow rate in case of flash boiling flow inside nozzle
  - Behaviors of velocity and pressure profile
  - Development of vapor profile along convergent-divergent nozzle

Charless.G., 1968; Abuaf et al., 1981; Wu et al., 1981

- **Numerical studies**

  - mixture model for flash boiling flow
  - thermal non-equilibrium phase change driven by pressure

Miad Yazdani et al, 2012; Yixiang Liao and Dirk Lucas, 2015;

EXPERIMENTAL BENCHMARK

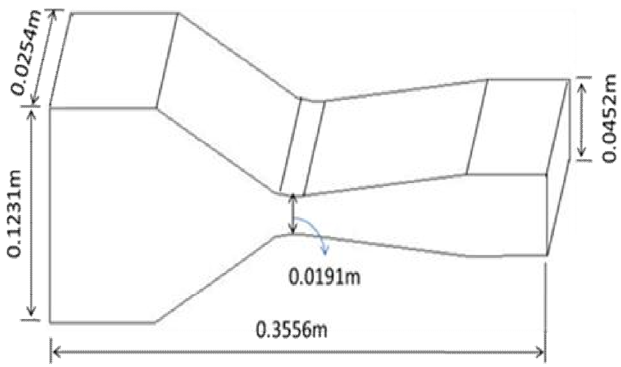

Charless. G. (1968)

Table. Operating conditions of Charless(1968)

Case	Upstream inlet pressure (Pa)	Mixture inlet temperature (K)	Inlet vapor mass fraction [-]
Case 1	145341.48	383.61	0.788
Case 2	135344.09	381.50	0.727
Case 3	185469.00	391.00	0.871
Case 4	181401.06	390.33	0.890
Case 5	189743.72	391.72	0.834
Case 6	178987.90	389.89	0.873
Case 7	184779.50	390.88	0.795
Case 8	158579.00	386.22	0.680
Case 9	134516.71	381.28	0.641

- Total inlet-pressure **(134 – 189 kPa)** and inlet vapor mas fraction **(0.6 – 0.9).**
- Atmospheric pressure at outlet

EXPERIMENTAL BENCHMARK

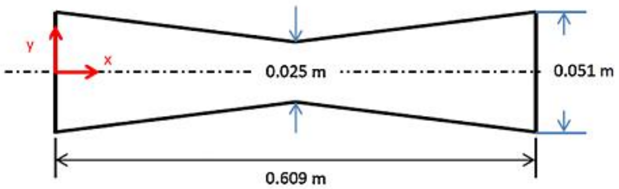

Abuaf et al.(1981)

Test	Upstream inlet pressure (kPa)	Inlet temperature (K)	Outlet pressure (kPa)	Saturaion pressure (kPa)
BNL309	555.9	422.25	402.5	464.8
BNL284	530	422.35	456	466
BNL273	573.5	421.85	442.1	459.8
BNL268	575.2	422.05	443	462.3
BNL304	577.7	422.15	441	463.5
BNL278	688.6	421.95	434.1	461
BNL296	764.9	421.95	432.6	461

- Total inlet-pressure **(530 – 764.9 kPa)** and **initial sub-cooled liquid** at inlet
- Saturation pressure depends on inlet temperature

NUMERICAL MODELLING

a/

b/

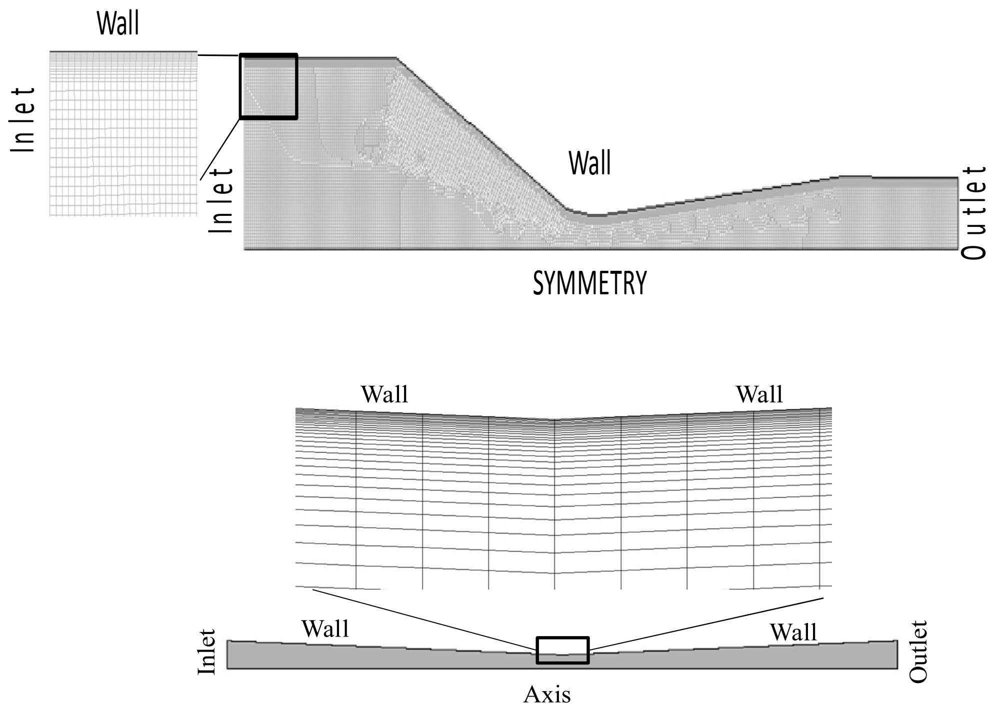

2D-axisymmetric approach

Figure. Mesh and boundary conditions in case of a/ Charless and b/ Abuaf et al

- quadratic cells with Local refinement
- Mesh sensitivity analysis - GCI

NUMERICAL MODELLING

FLUID DLOW / TURBULENCE MODEL

- Mass, momentum and energy conservation of mixture flow
- Approximation of slip velocity between two phases by Manninen et al.
- k-omega SST model is used

FLASH BOILING MODEL

$$\frac{\partial}{\partial t}\left(\alpha_v \rho_v\right) + \nabla \cdot \left(\alpha_v \rho_v \overrightarrow{V_v}\right) = \dot{m}_{lv} - \dot{m}_{vl}$$

Evaporation $T_l > T_{sat}$: $\dot{m}_{lv} = coeff \times \alpha_l \rho_l \frac{\left(T_l - T_{sat}\right)}{T_{sat}}$

Condensation $T_v < T_{sat}$: $\dot{m}_{vl} = coeff \times \alpha_l \rho_l \frac{\left(T_l - T_{sat}\right)}{T_{sat}}$

- Evaporation/condensation frequency $coeff = \frac{6}{d_b} \beta \sqrt{\frac{M}{2\pi R T_{sat}}} L \left(\frac{\alpha_v \rho_v}{\rho_l - \rho_v}\right)$

NUMERICAL MODELLING

- Evaporation driven by pressure from evaporation-condensation model FLUENT

- The Clausius Clapeyron equation yields the following formula as long as p^* and T* are close to the saturation condition

$$\left(P^* - P_{sat}\right) = -\frac{L}{T\left(v_v - v_l\right)}\left(T^* - T_{sat}\right)$$

- Hetz Knudsen equation

$$\dot{m}_{boil}\left[\frac{kg}{m^3 s}\right] = A_i \beta \sqrt{\frac{M}{2\pi R T_{sat}}}\left(P^* - P_v\right)$$

$A_i\left[m^{-1}\right] = \left(6\alpha_g\right)^{2/3}\left(\pi N_b\right)$ Interfacial area density. (Yixiang Liao and Dirk Lucas, 2015)

β accommodation coefficient for boiling delay and will be choosed by fitting experimental data

Saturation Pressure is defined as $P_v = P_{sat} + 0.195\rho k$ (Miad Yazdani et al, 2012)

with k is turbulent kinetic energy and ρ is mixture density

Results

Charless' Operating Conditions (1968)

Case	Upstream inlet pressure (Pa)	Mixture Model Mass Flow Rate (kg/s)	Experimental Data Mass Flow Rate (kg/s)	Relative Error (%)
Case 1	145341.48	0.133	0.128	4.0
Case 2	135344.09	0.128	0.128	0.0
Case 3	185469.00	0.161	0.150	6.4
Case 4	181401.06	0.156	0.144	8.0
Case 5	189743.72	0.166	0.159	4.7
Case 6	178987.90	0.156	0.143	8.2
Case 7	184779.50	0.167	0.159	5.0
Case 8	158579.00	0.156	0.156	0.4
Case 9	134516.71	0.136	0.138	2.1

Maximum error is 8.2% and minimum error is 0.01%

Results

Charless' Operating Conditions (1968)

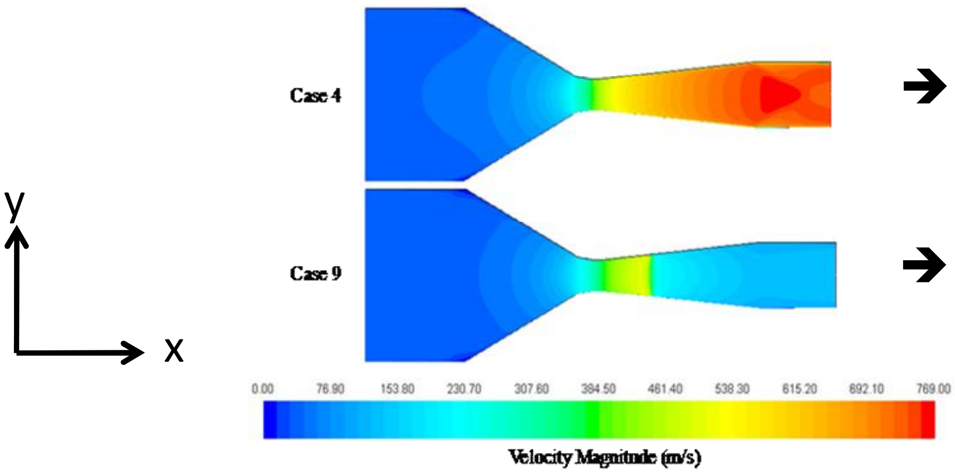

➔ Maximum pressure drop

➔ Minimum pressure drop

Figure: Velocity magnitude of mixture flow in nozzle of Case 4 (Upper) and Case 9 (Lower)

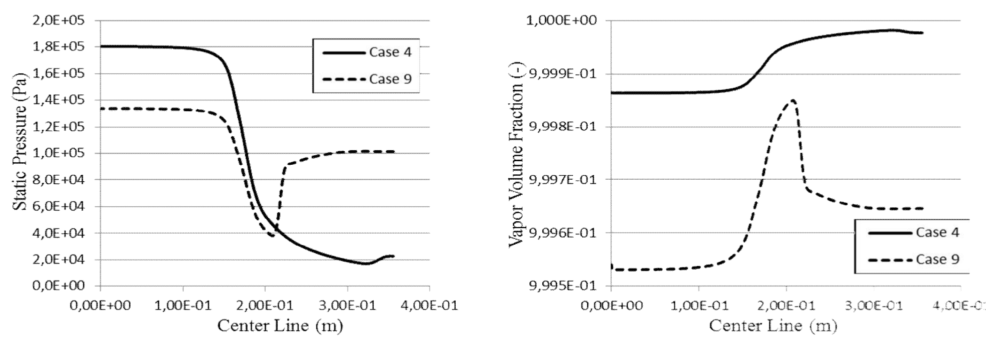

(a) Static pressure *(b) Vapor fraction*

Figure: Static pressure and vapor fraction along center line of nozzle

Results

Abuaf et al's Operating Conditions (1981)

Test	Numerical MFR (kg/s)	Experiment MFR (kg/s)	Relative error (%)
BNL309	8.5	8.4	1.1
BNL284	7.79	7.3	6.2
BNL273	9.3	8.7	6.4
BNL268	9.27	8.7	5.8
BNL304	9.1	8.8	3.2
BNL278	12.2	11.7	4.0
BNL296	13.9	13.1	5.7

- Maximum error is 6.4%
- Minimum error is 1.1%

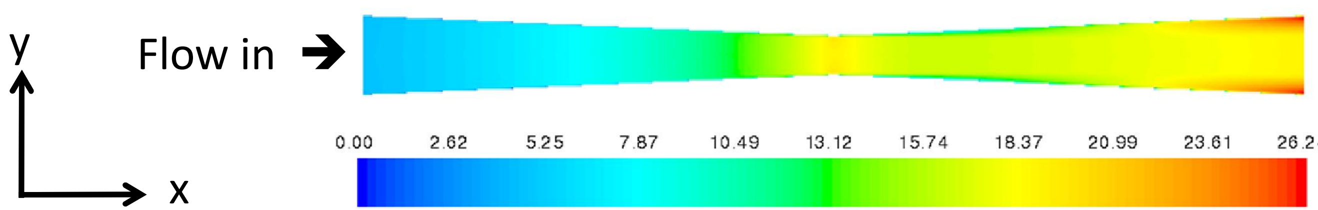

Figure: Velocity magnitude in BNL309

Results

Abuaf et al's Operating Conditions (1981)

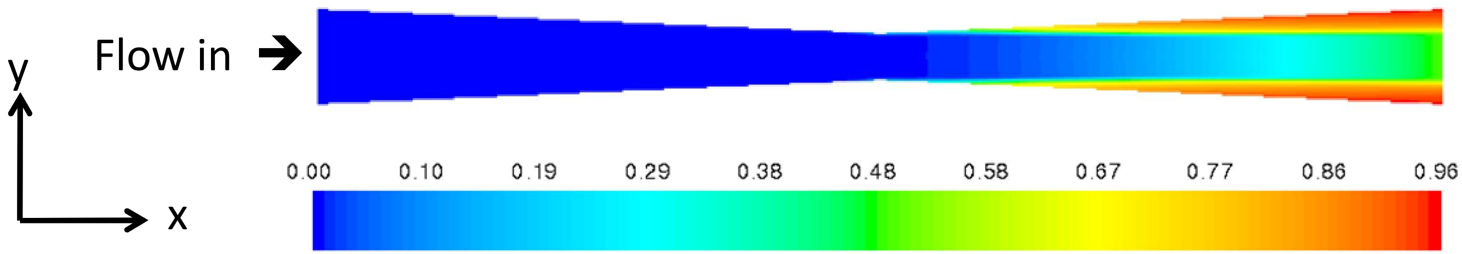

Figure. Vapor fraction distribution in BNL309

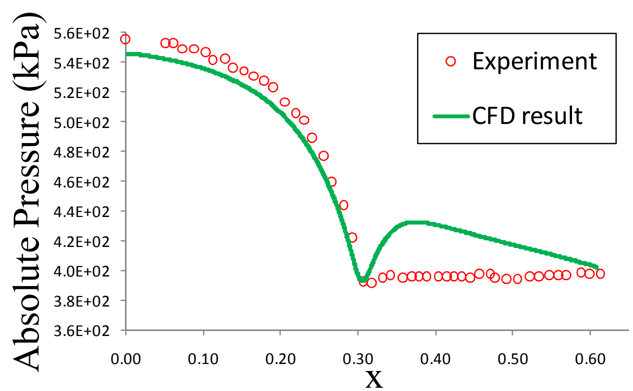

Figure . Absolute pressure along nozzle in BNL309

Results

Abuaf et al’s Operating Conditions (1981)

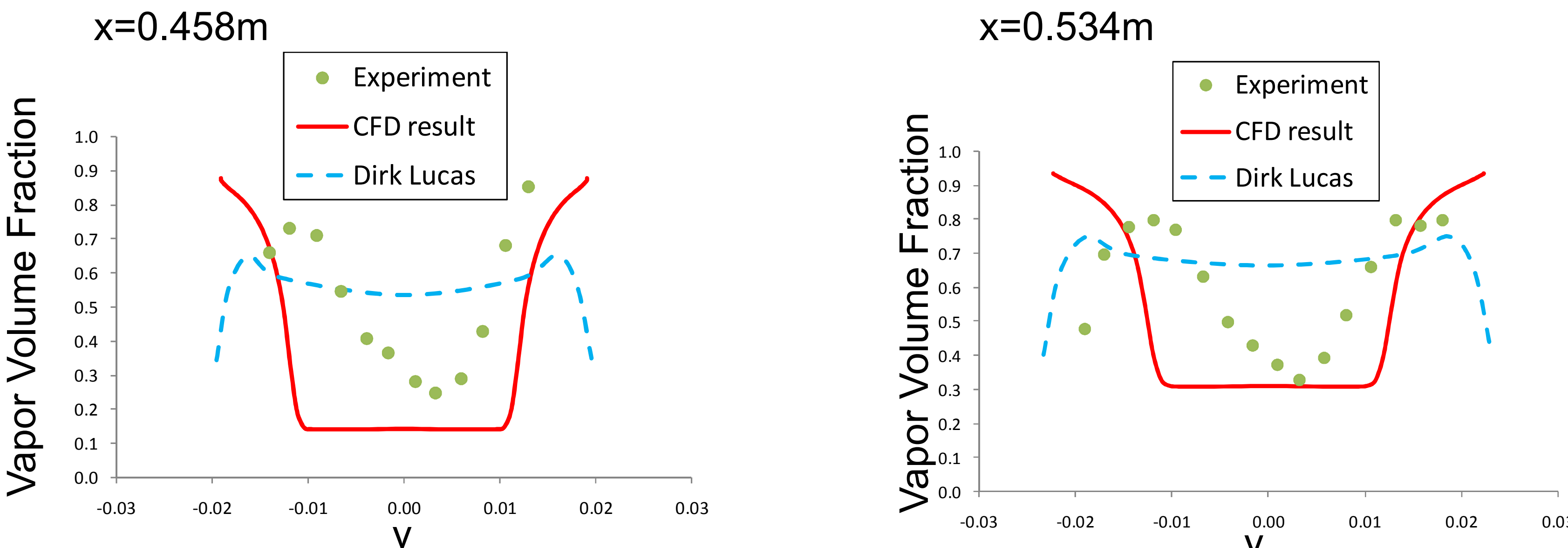

Figure . Vapor fraction profile at x=0.458m and x=0.534m in BNL309

- Reasons for discrepancies between CFD analysis and Experiment

  ○ Phenomenon near wall involves to bubble dynamics (coalesence, break-up and immigration of bubbles) which RANS models cannot perform.

Abuaf et al's Operating Conditions (1981)

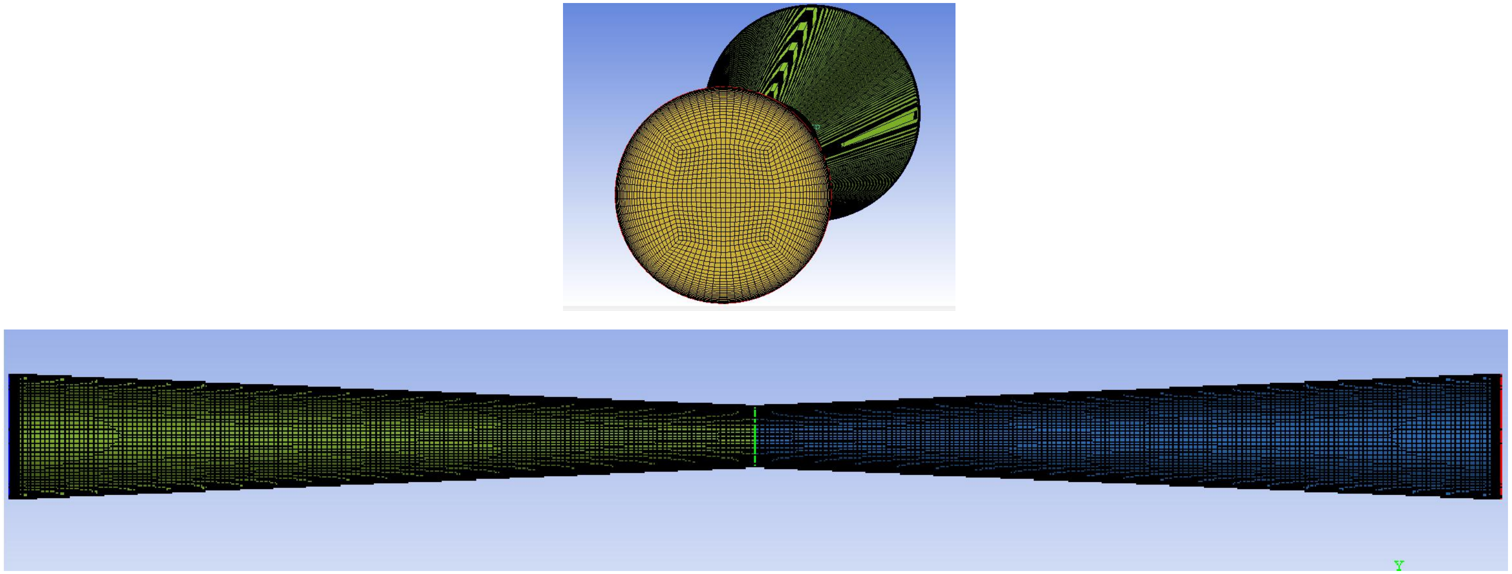

Figure. *3D* Mesh in case of Abuaf et al.(1981)

	2D-axisymmetric	3D Our Results	3D Lucas
Min Yplus	6	50	88
Max Yplus	16	210	259

3D Our Results Mesh of 843696 Elements → similar to 3D mesh in paper of Dirk Lucas

Results

Abuaf et al's Operating Conditions (1981)

	2D-axisymmetric	3D Our Results	3D Lucas	Experiment
Mass Flow Rate	8.8	8.66	8.4	8.8

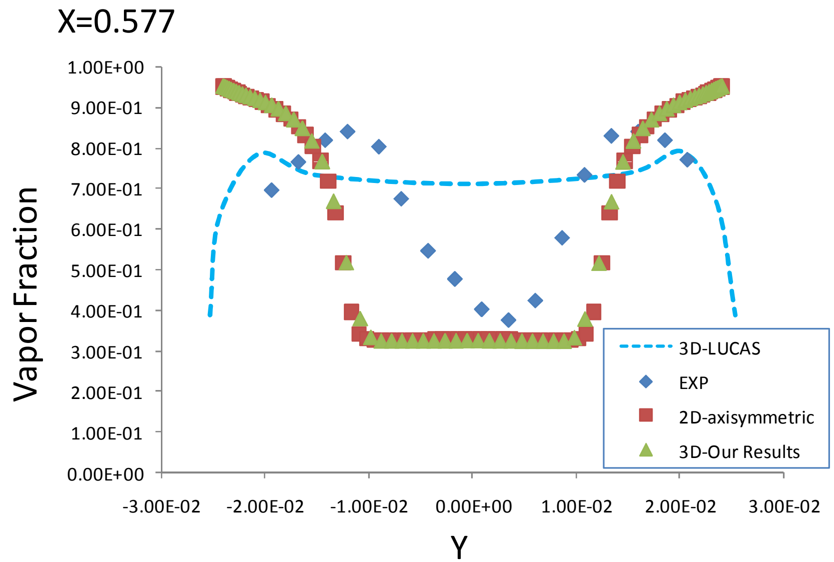

Results of 2D-axisymmetric model and 3D model are similar ➔ 2D-axisymmetric model can be used for further evaluation in this case

Final remarks

Conclusions

- Validation of CFD results using experimental data
- Analysis of local phenomenon inside nozzle (i.e. vapor profile, velocity profile and pressure distribution)
- Compare with other method for modeling flash boiling flow in nozzle
- Compare between 2D-axisymmetric model and 3D model to obtain useful model for industrial application

Future studies

- Study on different turbulent models
- Using this results for developing valve sizing formula (both of control valve and safety valve) in case of flash boiling flow

THANK YOU for YOUR ATTENTION!!!

NUMERICAL MODELLING

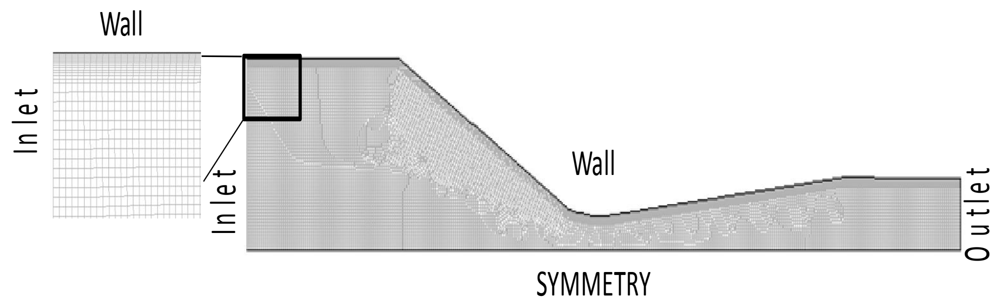

Figure. Mesh and boundary condition in case of Charless. G. (1968)

- The mesh is based on quadratic cells with skewness below 0.52
- Mesh sensitivity analysis is performed with mesh of 15751 elements (standard mesh) and mesh of 25457 elements (fine mesh) for all test cases.
  - Standard mesh is obtained with differences of mass flow rate between 2 meshes is 0.5%

Results

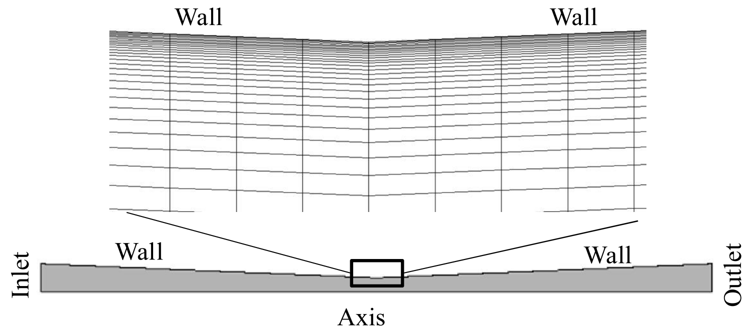

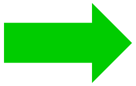

2D-axisymmetric approach

Figure. Mesh and boundary conditions in case of Abuaf et al.(1981)

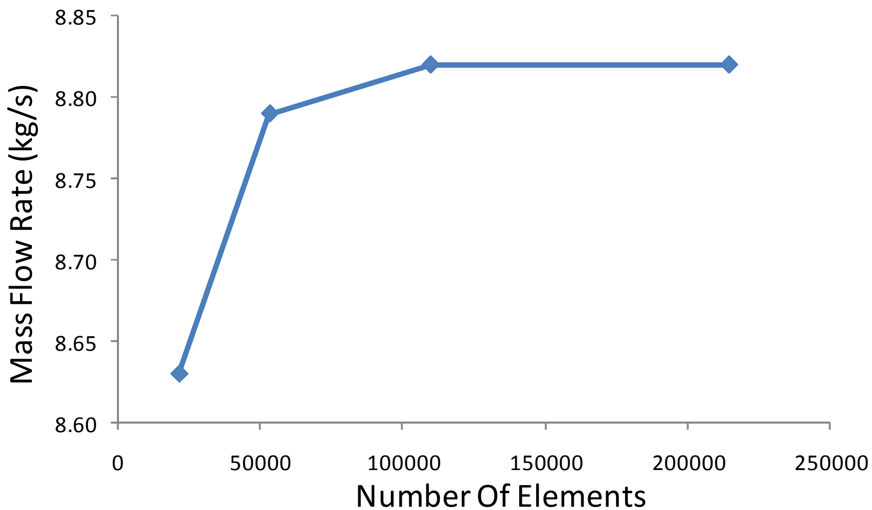

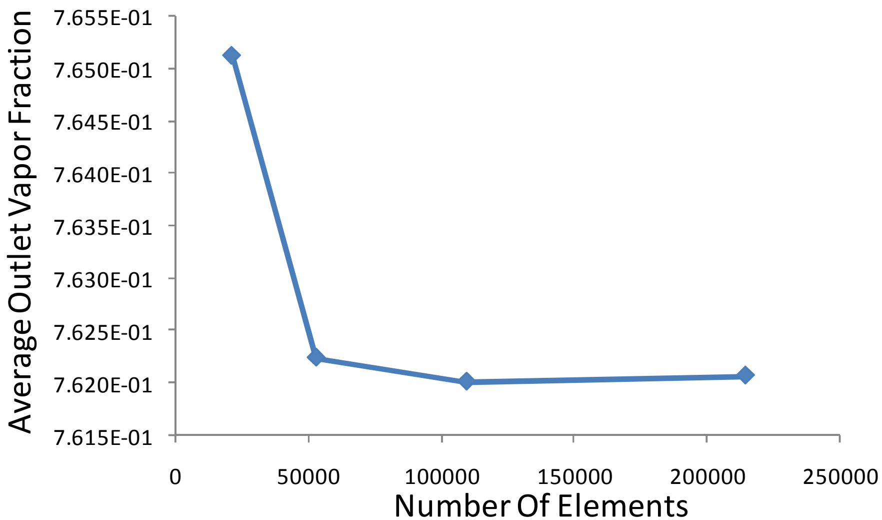

Figure. Grid analysis in case BNL309 of Abuaf et al.(1981)

Theoretical background

Mass, momentum and energy conservation of mixture model

Continuity equation

$$\frac{\partial \rho_m}{\partial t} + \nabla \cdot \left(\rho_m \vec{v}_m\right) = 0$$

Momentum conservation equation

$$\frac{\partial \left(\rho_m \vec{v}_m\right)}{\partial t} + \nabla \cdot \left(\rho_m \vec{v}_m \vec{v}_m\right) = -\nabla p + \nabla \cdot \left[\mu_m \left(\nabla \vec{v}_m + \nabla \vec{v}_m^T\right)\right] + \rho_m \vec{g} + \vec{F} + \nabla \cdot \left(\sum_{k=1}^{n} \alpha_k \rho_k \vec{v}_{dr,k} \vec{v}_{dr,k}\right)$$

Energy conservation equation

$$\frac{\partial \left(\sum_{k=1}^{n} \alpha_k \rho_k E_k\right)}{\partial t} + \nabla \cdot \sum_{k=1}^{n} \left(\alpha_k \vec{v}_k \left(\rho_k E_k + p\right)\right) = \nabla \cdot \left(k_{eff} \nabla T\right)$$

Theoretical background

Model of flash boiling flow

$$\frac{\partial}{\partial t}(\alpha_v \rho_v) + \nabla \cdot \left(\alpha_v \rho_v \overrightarrow{V_v}\right) = \dot{m}_{lv} - \dot{m}_{vl}$$

Evaporation $T_l > T_{sat}$: $\dot{m}_{lv} = coeff \times \alpha_l \rho_l \frac{(T_l - T_{sat})}{T_{sat}}$

Condensation $T_v < T_{sat}$: $\dot{m}_{vl} = coeff \times \alpha_l \rho_l \frac{(T_l - T_{sat})}{T_{sat}}$

Evaporation/condensation frequency $coeff = \frac{6}{d_b} \beta \sqrt{\frac{M}{2\pi R T_{sat}}} L \left(\frac{\alpha_v \rho_v}{\rho_l - \rho_v}\right)$

Model of flash boiling flow inside throttling device

$$\vec{v}_m\left[m\cdot s^{-1}\right]=\frac{\sum_{k=1}^{n}\alpha_k\rho_k\vec{v}_k}{\rho_m}$$ mass-averaged velocity

$$\rho_m\left[kg\cdot m^{-3}\right]=\sum_{k=1}^{n}\alpha_k\rho_k$$ mixture density

$$\mu_m\left[kg\cdot m^{-1}\cdot s^{-1}\right]=\sum_{k=1}^{n}\alpha_k\mu_k$$ mixture viscosity

$$E_k\left[kg\cdot m^{2}\cdot s^{-1}\right]$$ internal energy of phase k

$$k_{eff}\left[W\cdot m^{-1}\cdot K^{-1}\right]=\sum\alpha_k\left(k_k+k_t\right)$$ effective conductivity with

$$k_t\left[W\cdot m^{-1}\cdot K^{-1}\right]$$ turbulent thermal conductuvity